Interactive Propagation of Photosensitive Chemical Waves on Two Circular Routes

Satoshi Nakata,*,† Sayaka Morishima,† and Hiroyuki Kitahata‡

Department of Chemistry, Nara University of Education, Takabatake-cho, Nara 630-8528, Japan, and Department of Physics, Graduate School of Science, Kyoto University, Kyoto 606-8502, Japan

Received: November 27, 2005; In Final Form: January 24, 2006

The propagation of chemical waves in the photosensitive Belousov−Zhabotinsky (BZ) reaction was investigated using an excitable field composed of two rings in slight contact, which were drawn using computer software and then projected on a film soaked with BZ solution using a liquid-crystal projector. When the initial phase difference between the two chemical waves in the individual rings was smaller than a critical value, this initial value was maintained after collision of the chemical waves. However, when the initial phase difference was larger than this critical value, the phase difference converged to the same value after the second collision. The critical value increased with an increase in the thickness of the rings. These experimental results on the geometry of the excitable field are discussed in relation to the nature of chemical wave propagation. These results suggest that the photosensitive BZ reaction may be useful for creating spatiotemporal patterns that depend on the geometric arrangement of excitable fields.

Introduction

Experimental and theoretical studies on wave propagation on an excitable medium may help us not only to understand signal processing in biological systems[1] such as nerve impulses[2,3] but also to create novel methods for artificial processing such as image processing[4−7] and logic operations[8−13] based on a reaction−diffusion system. The Belousov−Zhabotinsky (BZ) reaction has been experimentally and theoretically investigated as an excitable and oscillatory chemical system.[14−16] The BZ reaction on a two-dimensional field, e.g., filter paper,[17,18] Nafion membrane,[19−21] glass filter,[22] or gel,[23,24] has been well-studied because the nature of wave propagation depends on the spatial condition of the excitable field, which can be prepared by cutting[17,20−23] or printing.[18] In such systems, however, it can be technically difficult to cut a two-dimensional field with a complex shape or a completely uniform shape and to regulate the number of chemical waves and their intervals.

A photosensitive experimental setup of the BZ reaction[4,25] makes it easier to create excitable fields with various geometries, which are drawn by computer software and then projected onto a filter membrane soaked with photosensitive BZ solution using a liquid-crystal projector.[13,26] In this case, light illumination produces bromide ion which inhibits the oscillatory reaction, i.e., the degree of excitability can be adjusted by changing the intensity of illumination. Therefore, the number of chemical waves and their locations can be spatiotemporally regulated by local illumination of unwanted waves for a short time.[13,27]

We have recently reported the nature of the collision of two chemical waves in the photosensitive BZ reaction on an excitable field (a figure-eight field composed of two equivalent circular rings) illuminated with a liquid-crystal projector.[28] When two chemical waves were generated on the figure-eight field (one chemical wave propagating in the same direction in each circle) as the initial condition, the location of the collision of the waves either was constant or alternated depending on the initial phase difference and the degree of overlap of the two circular rings.

In the present study, we examined the characteristic features of wave propagation and collision using the photosensitive BZ reaction in comparison with a theoretical prediction of the nature of wave propagation as the development of our previous study.[28] On a figure-eight reaction field with various ratios of the inner and outer radii, several experiments with various initial phase differences were performed for circular rings in slight contact with one another. The experimental results were well-reproduced by the theoretical model. We believe that the various characteristics of this interactive wave propagation can be produced by drawing a geometrical excitable field with a computer according to the mathematical prediction.

Theory

We discuss the nature of BZ wave propagation in a reaction field on the basis of related papers.[29−32] Müller et al.[29] and Noszticzius et al.[30−32] reported that wave propagation on a uniform reaction field may be regarded as involute, since the chemical wave propagates in a direction perpendicular to the wave front with a uniform velocity and the boundary has little effect on the velocity. We previously reported that the shape of the photosensitive chemical wave on a circular ring is well-approximated as involute of the circle.[28]

In the present article, we discuss interactive chemical wave propagation on a figure-eight field composed of two equivalent rings in slight contact, as schematically shown in Figure 1. The phase difference between two chemical waves ($\Delta\theta = \theta_R - \theta_L$) is defined in Figure 1a, where θ_L and θ_R are the angles corresponding to the positions of the waves on the left and right inner rings. Here, we consider the case where a chemical wave on the right ring passes through the intersection before the chemical wave on the left ring reaches the intersection. In this condition, there are two types of collision that depend on the initial phase difference ($\Delta\theta_0$) and R, which is the ratio between

* To whom correspondence should be addressed. Tel & fax: +81-742-27-9191. E-mail: nakatas@nara-edu.ac.jp.
† Nara University of Education.
‡ Graduate School of Science, Kyoto University.
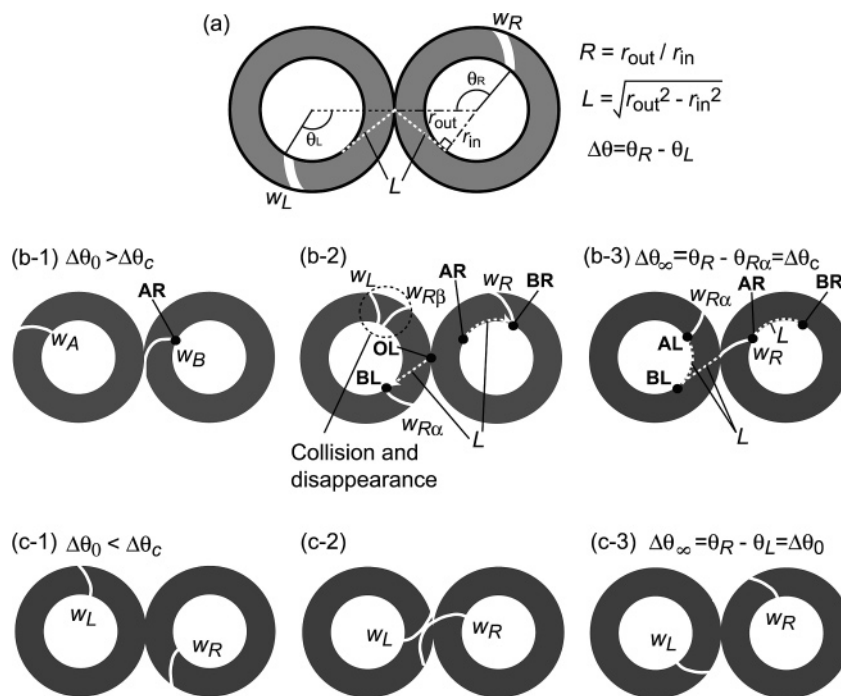
Figure 1. Schematic illustration of the propagation of two chemical waves (w_R and w_L) on a reaction field composed of two equivalent rings that are in slight contact with one another. (a) Definition of R, $\Delta\theta$, and L. Schematic illustration of characteristic collision patterns depending on the initial phase difference for (b) $\Delta\theta_0 > \Delta\theta_c$ and (c) $\Delta\theta_0 < \Delta\theta_c$.

the inner (r_{in}) and outer radii (r_{out}) of the two equivalent rings, i.e., $R = r_{out}/r_{in}$.

On the basis of the calculation in our previous paper,[28] we can derive a critical phase difference, $\Delta\theta_c$, which strongly affects the characteristic features of interactive wave propagation. When two rings are in slight contact, the path length, L, in Figure 1a is

$$L = \sqrt{r_{out}^2 - r_{in}^2} \qquad (1)$$

When the outer part of the chemical wave on the right ring (w_R) reaches the intersection of the two rings (see Figure 1b-1), θ_R is the phase of point **AR**, i.e., $L/r_{in} - \arccos(r_{in}/r_{out})$, which corresponds to the phase difference between the inner and outer boundaries of a single circular ring.[28] w_R is equivalently diverged to the lower ($w_{R\alpha}$) and upper ($w_{R\beta}$) directions on the left ring from the intersection. We suppose that w_L and $w_{R\beta}$ collide and disappear on the left ring if $\Delta\theta_0$ is not less than $\Delta\theta_c$. In contrast, w_R and $w_{R\alpha}$ remain on the right and left rings, respectively (Figure 1b-2). While $w_{R\alpha}$ propagates from point **OL** to **BL**, w_R propagates from **AR** to **BR**. The distance between **OL** and **BL** is L; θ_R proceeds L/r_{in}, while $w_{R\alpha}$ propagates from points **OL** to **BL**. Thus, when w_R is at point **BR**, $w_{R\alpha}$ is at point **BL**. The phase is derived as $\theta_R = 2L/r_{in} - \arccos(r_{in}/r_{out})$ and $\theta_L = \arccos(r_{in}/r_{out})$, which leads that the phase difference between the two waves

$$\Delta\theta = 2L/r_{in} - \arccos(r_{in}/r_{out}) - \arccos(r_{in}/r_{out}) = \\ 2[\sqrt{R^2 - 1} - \arccos(1/R)]$$

Considering the second collision, while $w_{R\alpha}$ propagates from point **AL** to **BL**, w_R proceeds the same distance, L, along the inner boundary of the right ring. In this stage, $\theta_R = 2L/r_{in} - \arccos(r_{in}/r_{out})$ at point **AR** and $\theta_L = \arccos(r_{in}/r_{out})$ at point **AL**. The second collision occurs between w_R and $w_{R\alpha}$, and further collisions occur repetitively. $w_{R\alpha}$ proceeds from **AL** to **BL**, while w_R proceeds from **AR** to **BR**. Therefore, $\Delta\theta$

converges to $\Delta\theta_\infty$ after the second collision. Thus, $\Delta\theta_\infty = \Delta\theta_c$ for every $\Delta\theta_0$ which is not less than $\Delta\theta_c$ (Figure 1b-3), and $\Delta\theta_c$ is obtained as

$$\Delta\theta_c = 2[\sqrt{R^2 - 1} - \arccos(1/R)] \qquad (2)$$

The other type of behavior is generated when $\Delta\theta_0 < \Delta\theta_c$, as shown in Figure 1c-1. Under this initial condition, the chemical wave translated from the right ring collides with w_L before $w_{R\alpha}$ touches the inner boundary of the left ring (Figure 1c-2). w_L partly disappears because of the collision, but w_L around the inner boundary is maintained after the collision (Figure 1c-3). Therefore, w_R and w_L do not change after the collision, i.e., $\Delta\theta$ is maintained at $\Delta\theta_0$. Thus, the converged phase difference after the collision ($\Delta\theta_\infty$) is equal to $\Delta\theta_0$.

Considering both types of collision, $\Delta\theta_\infty$ is written as

$$\Delta\theta_\infty = \begin{cases} \Delta\theta_c & \text{if } \Delta\theta_0 > \Delta\theta_c \\ \Delta\theta_0 & \text{if } \Delta\theta_0 < \Delta\theta_c \end{cases} \qquad (3)$$

where $\Delta\theta_c$ is a monotonically increasing function of R (see eq 2), as shown in Figure 2a. Therefore, the relationship between $\Delta\theta_0$ and $\Delta\theta_\infty$ is schematically shown in Figure 2b.

Experimental Section

Ru(bpy)$_3$Cl$_2$, which was purchased from Sigma-Aldrich (St. Louis, MO), was used as a catalyst for the photosensitive BZ reaction. The BZ solution consisted of [NaBrO$_3$] = 0.45 M, [H$_2$SO$_4$] = 0.3 M, [CH$_2$(COOH)$_2$] = 0.2 M, [KBr] = 0.05 M, and [Ru(bpy)$_3$Cl$_2$] = 1.7 mM. A cellulose nitrate membrane filter (Advantec, A100A025A, diameter of the membrane = 25 mm) with a pore size of 1 μm was homogeneously soaked in BZ solution (5 mL) for about 1 min. The soaked membrane was gently wiped with another pure filter paper to remove excess solution and placed on a glass plate (77 × 52 × 1.3 mm^3). The surface of the membrane filter was completely covered with 1 mL silicone oil (Wako, WF-30) to prevent it from drying and

Photosensitive Chemical Waves

J. Phys. Chem. A, Vol. 110, No. 10, 2006 **3635**
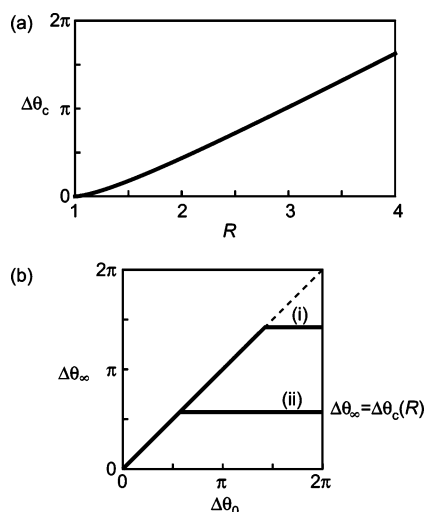
Figure 2. Theoretical results for (a) $\Delta\theta_c$ depending on R and (b) schematic illustration of the relationship between the initial phase difference, $\Delta\theta_0$ and the final phase difference $\Delta\theta_\infty$, based on eqs 2 and 3. (i) and (ii) in (b) correspond to a larger and smaller R, respectively. $\Delta\theta_\infty$ is equal to $\Delta\theta_c$ when $\Delta\theta_0$ is greater than $\Delta\theta_c$, and $\Delta\theta_\infty$ is equal to $\Delta\theta_0$ when $\Delta\theta_0$ is smaller than $\Delta\theta_c$.
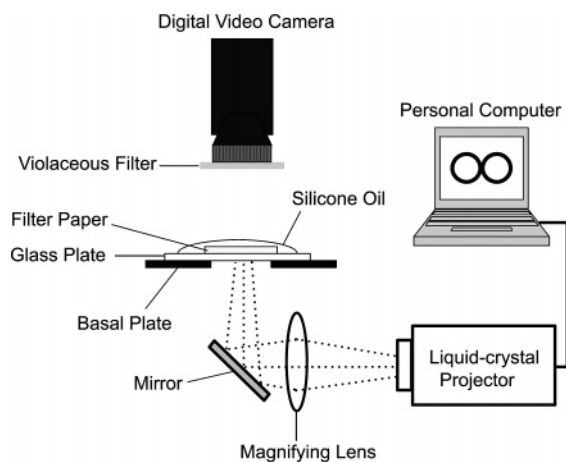
Figure 3. Schematic illustration of the experimental system based on the photosensitive BZ reaction.

to protect it from the influence of oxygen in air. The experiments were carried out in an air-conditioned room at 298 K, at which the reaction medium showed no oscillation and exhibited almost constant behavior in wave propagation for approximately 30 min.

The medium was illuminated from below as schematically shown in Figure 3. The high-pressure mercury bulb of a liquid-crystal projector (Mitsubishi LVP-XL8) was used as a light source, the spatial intensity distribution was controlled by a personal computer, and a magnifying lens was used to adjust the focus. The black and white picture created by the liquid-crystal projector served as an illumination mask to create the appropriate boundary, and the light intensities for the black and white regions were 4.0×10^2 lx and 1.7×10^4 lx. As for the status of the contact of two equivalent circular rings in a figure-eight, the distance between the centers of the two rings was nearly equal to $2r_{out}$ (r_{out} = radius of the outer ring), i.e., the two rings were just slightly in contact with one another. We examined three figure-eight fields with different ring thicknesses, i.e., $R = 1.32$ for thin rings, $R = 1.86$ for mid-thickness rings, and $R = 3.73$ for thick rings. In these rings, r_{in} was varied under constant r_{out} (3.7 ± 0.1 mm). The velocity of the chemical wave

at the inner boundary of the circle was maintained at ca. 0.06 mm s^{-1} and was almost independent of r_{in}.

As for adjustment of the number and direction of the chemical waves, one chemical wave was initially generated in each ring in the same direction (clockwise), so that the chemical wave in the right ring reached the intersection before that in the left ring. To prepare a unidirectional chemical wave on each ring, the following processes were performed: (1) Several chemical waves were initially generated on the excitable field under no illumination, i.e., dark condition. (2) When the illumination except for the dark area of the figure-eight was started, the chemical waves disappeared in the illuminated area but remained in the figure-eight. (3) Upon local illumination of unwanted waves for 1 s, the illuminated waves disappeared, and finally, one wave continued to propagate in each ring. Therefore, a unidirectional chemical wave was made in each ring.

The experiments were monitored from above with a digital video camera (Sony DCR-VX700) and recorded on videotape. A blue optical filter (Asahi Techno Glass, V-42) with a maximum transparency at 410 nm was used to enhance the image of the green-colored chemical waves, which correspond to the oxidized state, [Ru(bpy)$_3$]$^{3+}$. The light intensity at the illuminated part was measured with a light intensity meter (Asone, LX-100).

Results and Discussion

Figure 4 shows snapshots of wave propagation on rings of different thicknesses. For the thin rings at $R = 1.32$, two chemical waves first collided in the left ring and completely disappeared (snapshot 2 in Figure 4a). A second collision occurred between the chemical wave in the right ring, and another propagated from the right ring to the left ring (snapshot 2 in Figure 4a). The second collision was observed in the left ring near the intersection (snapshot 3 in Figure 4a), and the chemical wave in the left ring continued to propagate after the collision. The location of the collision converged near the intersection after the second collision. Thus, thin rings tended to show case (c) in Figure 1.

For the thick rings at $R = 3.73$, the first collision was observed in the left ring near the intersection (snapshot 2 in Figure 4b). The inner part of the chemical wave in the left ring then continued to propagate after the collision. The location of the collision and $\Delta\theta$ were maintained after the collision (snapshot 3 in Figure 4b). Thus, thick rings tended to show case (b) in Figure 1.

For mid-thickness rings at $R = 1.86$, two characteristic types of collision were clearly observed depending on $\Delta\theta_0$, as seen in Figures 4c and d: collision near the intersection (snapshot 2 in Figure 4c) and the first collision in the left ring except for the intersection (snapshot 2 in Figure 4d). In the former case, the inner part of the chemical wave in the left ring remained after the collision, i.e., $\Delta\theta$ values of the left and right rings were maintained after the collision (snapshots 1 and 3 in Figure 4c). In the latter case, the chemical wave in the left ring, which was translated from the right ring after the first collision, collided with the chemical wave in the right ring (snapshots 2 and 3 in Figure 4d), and the location of this collision converged near the intersection after the second collision. Thus, both cases (c) and (b) which correspond to (c) and (d) in Figure 4 were observed for mid-thickness rings.

Figure 5 shows $\Delta\theta_\infty$ depending on $\Delta\theta_0$ for different R. On the basis of eqs 2 and 3, $\Delta\theta_\infty$ was calculated for $R = 1.32$, 1.86, and 3.73 and drawn as a thin line for comparison with the experimental results. For thin rings ($R = 1.32$), $\Delta\theta_\infty$ was a
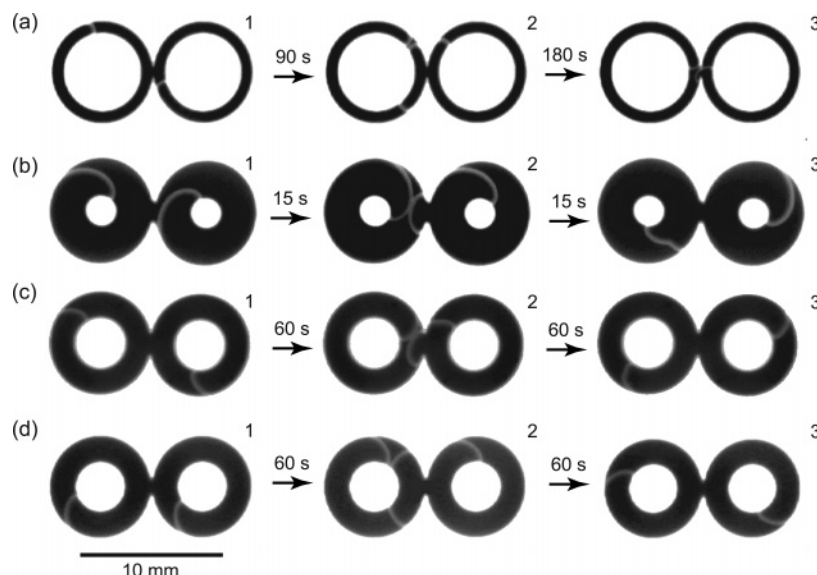
Figure 4. Top view of snapshots of wave propagation on rings at (a) $R = 1.32$ (thin rings), (b) $R = 3.73$ (thick rings), and (c,d) $R = 1.86$ (mid-thickness rings). Time intervals between the individual snapshots are indicated above the arrows. $\Delta\theta_0 =$ (a) 0.49π, (b) 0.62π, (c) 0.06π, and (d) 0.91π rad.
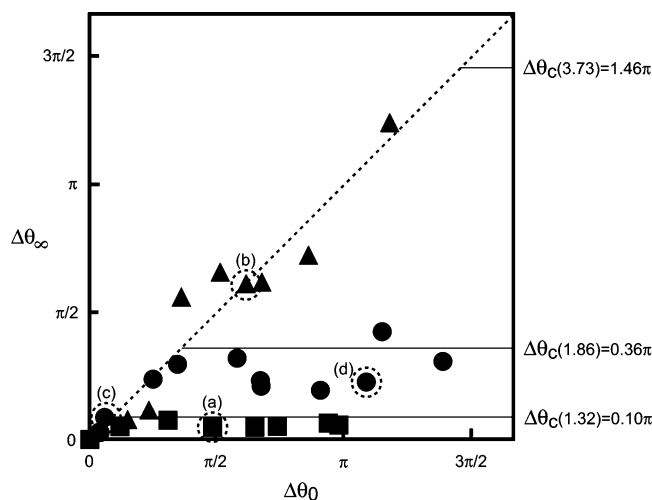
Figure 5. Experimental results for the dependence of the converged phase difference ($\Delta\theta_\infty$) on the initial phase difference ($\Delta\theta_0$) for $R = 1.32$ (square), 1.86 (circle), and 3.73 (triangular). Values of 0.1π, 0.36π, and 1.46π rad and the thin lines were obtained on the basis of eqs 2 and 3 at $R = 1.32$, 1.86, and 3.73, respectively. a, b, c, and d marked in Figure 5 correspond to those in Figure 4, respectively.

small positive value at $(0.06 \pm 0.01)\pi$ for every $\Delta\theta_0$, i.e., the location of the collision converged near the intersection almost independent of $\Delta\theta_0$. For thick rings ($R = 3.73$), $\Delta\theta_\infty$ clearly increased with $\Delta\theta_0$ and could be linearly approximated by $\Delta\theta_c = 1.11 \times \Delta\theta_0$ (contribution ratio = 0.75). For mid-thickness rings ($R = 1.86$), $\Delta\theta_\infty$ linearly increased with $\Delta\theta_0$ at $\Delta\theta_0 < 0.3\pi$, but $\Delta\theta_\infty$ was almost maintained at $(0.29 \pm 0.08)\pi$ at $\Delta\theta_0 > 0.3\pi$. Although two rings were only in slight contact with one another on the image created by computer software, the actual chemical waves propagated to the other ring via the bright region near the boundary of the intersection before passing through the intersection, and therefore, the experimental results for $\Delta\theta_\infty$ were lower than those predicted by the calculation. However, the experimental results regarding the relationship between $\Delta\theta_0$ and $\Delta\theta_\infty$ as a function of R are well-reproduced by the relationship based on eqs 2 and 3. We have also confirmed that the characteristics of chemical wave propagation

on a figure-eight field depending on R and $\Delta\theta_0$ are qualitatively reproduced by a numerical simulation based on the Oregonator model for the photosensitive BZ reaction, according to our previous calculation[28] (data not shown).

Conclusion

The nature of wave propagation and collision in the photosensitive BZ reaction on an excitable figure-eight field illuminated with a liquid-crystal projector was demonstrated. There are two types of wave propagation with collision between two chemical waves, i.e., a converged phase difference ($\Delta\theta_\infty$) determined by the initial value ($\Delta\theta_0$) and $\Delta\theta_\infty$ independent of $\Delta\theta_0$ but determined by the critical value ($\Delta\theta_c$), and $\Delta\theta_c$ depends on the thickness of the ring (R). These features of wave propagation involving collision are approximately consistent with a mathematical consideration of the shortest path of the chemical wave. These results suggest that the various characteristics of the spatiotemporal pattern in the photosensitive BZ reaction, which can be adjusted by illumination, are possible to create on the basis of the mathematical prediction.

References and Notes

(1) Winfree, A. T. *The Geometry of Biological Time*; Springer: Berlin, 1980.

(2) Hall, Z. W., Ed. *Molecular Neurobiology*; Sinauer: Sunderland, MA, 1992.

(3) Murray, J. D. *Mathematical Biology*; Springer: Berlin, 1989.

(4) Kuhnert, L. *Nature (London)* **1986**, *319*, 393.

(5) Kuhnert, L.; Agladze, K. I.; Krinsky, V. I. *Nature (London)* **1989**, *337*, 244.

(6) Rambidi, N. G.; Shamayaev, K. E.; Peshkov, G. Y. *Phys. Lett. A* **2002**, *298*, 375.

(7) Sakurai, T.; Mihaliuk, E.; Chirila, F.; Showalter, K. *Science* **2002**, *296*, 2009.

(8) Tóth, A.; Showalter, K. *J. Chem. Phys.* **1995**, *103*, 2058.

(9) Steinbock, O.; Kettunen, P.; Showalter, K. *J. Phys. Chem.* **1996**, *100*, 18970.

(10) Motoike, I.; Yoshikawa, K. *Phys. Rev. E* **1999**, *59*, 5354.

(11) Ichino, T.; Igarashi, Y.; Motoike, N. I.; Yoshikawa, K. *J. Chem. Phys.* **2003**, *118*, 8185.

(12) Gorecka, J.; Gorecki, J. *Phys. Rev. E* **2003**, *67*, 067203.

(13) Nagahara, H.; Ichino, T.; Yoshikawa, K. *Phys. Rev. E* **2004**, *70*, 036221.

(14) Zaikin, A. N.; Zhabotinsky, A. M. *Nature (London)* **1970**, *225*, 535.

(15) Field, R. J., Burger, M., Eds. *Oscillations and Traveling Waves in Chemical Systems*; Wiley: New York, 1985.

(16) Kapral, R., Showalter, K., Eds. *Chemical Waves and Patterns*; Kluwer Academic: Dordrecht, 1995.

(17) Lázár, A.; Noszticzius, Z.; Försterling, H.-D.; Nagy-Ungvárai, Z. *Physica D* **1995**, *84*, 112.

(18) Steinbock, O.; Kettunen, P.; Showalter, K. *Science* **1995**, *269*, 1857.

(19) Winston, D.; Arora, M.; Maselko, J.; Gáspár, V.; Showalter, K. *Nature (London)* **1991**, *351*, 132.

(20) Iguchi, Y.; Takitani, R.; Miura, Y.; Nakata, S. *Rec. Res. Devel. Pure Appl. Chem.* **1998**, *2*, 113.

(21) Motoike, N. I.; Yoshikawa, K,; Iguchi, Y.; Nakata, S. *Phys. Rev. E* **2001**, *63*, 036220.

(22) Agladze, K.; Aliev, R. R.; Yamaguchi, T.; Yoshikawa, K. *J. Phys. Chem.* **1996**, *100*, 13895.

(23) Aliev, R. R.; Agladze, K. I. *Physica D* **1991**, *50*, 65.

(24) Yoshida, R.; Takahashi, T.; Yamaguchi, T.; Ichijo, H. *J. Am. Chem. Soc.* **1996**, *118*, 5134.

(25) Kádár, S.; Amemiya, T.; Showalter, K. *J. Phys. Chem. A* **1997**, *101*, 8200.

(26) Gorecki, J.; Yoshikawa, K.; Igarashi, Y. *J. Phys. Chem. A* **2003**, *107*, 1664.

(27) Amemiya, T.; Kádár, S.; Kettunen, P.; Showalter, K. *Phys. Rev. Lett.* **1996**, *77*, 3244.

(28) Kitahata, H.; Yamada, A.; Nakata, S.; Ichino, T. *J. Phys. Chem. A* **2005**, *109*, 4973.

(29) Müller, S. C.; Plesser, T.; Hess, B. *Physica D* **1987**, *24*, 87.

(30) Volford, A.; Simon, P. L.; Farkas, H.; Noszticzius, Z. *Physica A* **1999**, *274*, 30.

(31) Lázár, A.; Noszticzius, Z.; Farkas, H.; Försterling, H. D. *Chaos* **1995**, *5*, 443.

(32) Lázár, A.; Försterling, H.-D.; H. Farkas, Simon, P.; Volford, A.; Nosizticzius, Z. *Chaos* **1997**, *7*, 731.